A Markov-Transition Model for Cascading Failures in Power Grids

Zhifang Wang, *Member, IEEE,* Anna Scaglione, *Fellow, IEEE,* and Robert J. Thomas *Life Fellow, IEEE*

***Abstract*—The electric power grid is a complex critical infrastructure network. Its inter-connectivity enables long-distance transmission of power for more efficient system operation. The same inter-connectivity, however, also allows the propagation of disturbances. In fact, blackouts due to cascading failures occur because of the intrinsic electrical properties of this propagation and physical mechanisms that are triggered by it. In this paper we propose a stochastic Markov model, whose transition probabilities are derived from a stochastic model for the flow redistribution, that can potentially capture the progression of cascading failures and its time span. We suggest a metric that should be monitored to expose the risk of failure and the time margin that is left to perform corrective action. Finally we experiment with the proposed stochastic model on the IEEE 300 bus system and provide numerical analysis.**

I. Introduction

In this paper we develop a stochastic model to capture the progression of cascading failures in power grids. During the past decade a great deal of research effort has been devoted to studying the vulnerability of the power grid. There are two main lines of research: one focusing on *static failure models*, and one on *dynamic failure models*.

A. Static Failure Analysis

Studies using static failure models focus on the topological robustness of the grid, primarily gauging how the network connectivity changes after failures (or intentional attacks) on its nodes or links. The work by Rosas-Casals, Valverde, Solé et al. (2007) (see [1] and [2]) numerically examined the impact of node removals on the system global connectivity, and analytically evaluated the critical threshold of node removals to fragment a power grid network. This work related the topology robustness of a power grid network with its node degree distribution, assumed to be Geometric (or equivalently Exponential). Later, Wang, Scaglione, and Thomas (2010), improved the nodal degree model, showing excellent fit with a mixture distribution, sum of a truncated geometric random variable and an irregular discrete random variable [3]. Interestingly, the power grid is even more vulnerable to disconnection under this more realistic nodal degree distribution model. Xiao and Yeh (2010) [4] also studied the problem of cascading link failures in power networks using percolation theory. However, the power grid network has been incorrectly modeled as a random geometric graph. Recently, Hines, Cotilla-Sanchez, *et al.* (2011) [5] performed blackouts simulations, on several realistic power grid networks, under different attack strategies such as random attack, degree-attack, max or min-traffic attack, and tried to identify critical buses in terms of topology vulnerability by examining the attack impacts. They compare the simulation results with the predictions of other models, but do not provide an analytical static failure model, other than direct simulation. [5] also proposed that power grids may exhibit the *critical slowing down* phenomenon, which can be detected as a noticeable increase in the correlation of some phase angle or system frequency, that is a suitable risk indicator for the advent of a cascading blackouts.

Z. Wang and A. Scaglione are with the Department of Electrical and Computer Engineering, University of California, Davis, CA 95616 USA, e-mail: {zfwang, ascaglione}@ucdavis.edu.

R. J. Thomas is with the School of Electrical and Computer Engineering, Cornell University, Ithaca, NY 14850 USA, e-mail: rjt1@cornell.edu.

B. Dynamic Overload Failure Analysis

Analysis based on static-failure approaches reveals intrinsic vulnerabilities of the power grid network, but does not describe the evolution of system-wide blackouts, which is what dynamic failure analysis does.

To this end, the analysis incorporates triggering events, load flow re-distribution models, subsequent events of line-overload, all aimed at modeling the propagation of breakdowns in the network. In a nutshell, what differentiate dynamic models is the mechanism that governs the re-distribution of flows after failures and the overloading of lines.

The literature is divided in two main categories: one based on graph theory analysis and one using power grid analysis, often including an economic power dispatch after each failure, i.e., the linear OPF (optimal power flow).

1) Graph theoretic approaches: Motter and Lai (2002) proposed a model to study cascading overload failures in a power grid provoked by single intentional attacks [6]. Following Holme and Kim in [7], Motter and Lai assumed that every node pair in the power grid network exchanges some flow along the shortest path connecting them. Therefore, the load at a node matches its so called *betweenness*, measured as the total number of shortest paths passing through the node. Considering a node capacity limit, nodes can exceed such limit and when they fail, the flow is redistributed. Under some conditions, this may cause new nodes to become overloaded and their failures continue to propagate, producing a cascading phenomenon. Crucitti, Latora, and Marchiori (2004) modified the Motter-Lai cascading model in two ways[8]: (1) the overloaded nodes are not removed from the network, instead, the flow passing through them has progressively worse efficiency, due to congestion; (2) the damage caused by the cascading failures is quantified in terms of network efficiency, instead of being measured as the size of remaining connected component. These cascading models have been studied testing them on real-world network topologies, for the Internet and the North American power grid, as well as on random topologies, for example, Watts-Strogatz Small-world graphs, Kleinberg scale-free network model, and the Erdös-Rényi random graphs (see

[9] [10]). The conclusion drawn from this model is that the heterogeneity of load distribution in a network makes it particularly vulnerable to cascading failures which can be triggered by breaking down a single key node. In a similar vein, Wang and Rong (2009) [11] proposed a cascading model where the initial load setting on each bus is $L_j = \left(k_j \sum_{m\in\Gamma_j} k_m\right)^{\alpha}$ with k_j being node j degree and and Γ_j being the immediate neighboring set of node j, and α a tunable parameter; if one node is attacked and fails, its load will be proportionally redistributed to all its neighbors. However, the assumptions of load setting as well as flow distribution have no physical connection to the mechanism of realistic power grid operation. This model leads to the conclusion that the attack on the buses with the lowest loads may be more harmful than the attack on those with the highest loads.

2) Models based on realistic power flows: Dobson, Carresras *et al.* (2001) included the physical modeling of a power grid network in [12] to study the cascading process. They defined an initial model to probe the complex dynamics of power grid blackouts, that consists of a linearized DC power flow model for power flow dispatch.The power flow redispatch after node or line failures is realized as a deterministic optimization (LOPF) to minimize the change in generation or load shedding subject to system constraints, emulating the re-dispatch of energy generation that are part of normal system operations. Later Carreras, Karamitsos, Bao *et al.* (see [13] [14] [15]) adopted similar models as in [12]. Carreras, Lynch *et al.* (2002) used the power blackouts model of [12] to identify the critical points and transitions for cascading blackouts, based on a tree-topology network and the IEEE 118-bus network [13]. Karamitsos and Orfanidis (2006) applied the model from [12] to analyze power grid blackouts in simple networks with ring or tree topology [14]. Bao, Cao, *et al.* gave a similar power grid blackouts model as that in [13] except that it allows instantaneous line overload and the tripping of a line is only caused by accumulative effect of overload[15]. The authors also defined *power flow entropy* to quantify the heterogeneity of power flow distribution in a network and experiments cascading failures in a small-world 300-node system and the IEEE 300-bus system.

3) Stochastic modeling: A few authors have considered stochastic modeling. Dobson, Carreras and Newman (2005) [16] analyzed the line trips data of several blackouts in the US, and found that, the branching process model can provide a good fit for the cumulative number of line trips. Branching processes are useful to model population growth: each individual in one generation produces some random number of individuals in the next generation.

The graph theoretic approaches we surveyed use models that are appropriate for communication or vehicular networks. Information packets and vehicles can switch their route, and they preferentially choose shorter paths. And the nodes in such a network can easily switch roles as traffic generator or receiver. The flows in an electric power grid network obey Kirchhoff's Voltage/Current laws (KVL and KCL) and Ohm's law [17].The conservation of flows can be viewed as an equivalent constraint as Kirchhoff's circuit law. However, Kirchhoff's voltage law and Ohm's law are unique for a electric circuit network. Another distinction is that nodes in a power grid (frequently called *buses*) are divided in three classes: generators, loads and intermediate nodes. It does not make sense to interchange them.

While the class of models using economic dispatch after each failure is consistent with the physical reality of electrical power grids flows, the optimal power flow model, as shown in [12], may not be an appropriate approach to simulate the flow re-distribution process during the cascading failures. Although the cascading process in a power grid starts from isolated random contingencies, the root reason for the spreading of failures may lie in some intrinsic weakness of the network or some hidden failures, which go un-detected and therefore do not lead to timely corrective action. During the escalation of cascading failures, hundreds of lines are switched off in less than an hour period, and usually there is not enough time for planning any optimized generation re-dispatch or load-shedding. Only local transient controls are engaged, like the Generation Governor Control (GGC). Also, including the OPF in the simulation model is somewhat self-contradictory: on the one hand, it makes a necessary adjustment in generation and performs load shedding, in order to avoid line overloads after line outages; on the other hand, the job is left somewhat unfinished, since the OPF used does not perfectly depresses the flows well below the line capacity limits. Instead, some chance is left for additional overloads and line trips, so as to model the following stages.

Another common drawback in the prior art is the inability to capture the evolution process of cascading failures with regard to time since they only describe the cascading process in network state stages.

C. Our Contribution

In this paper we propose a stochastic model based on Markov transition of the power grid state, which incorporates the uncertainties in the system load settings and the corresponding generation and line flows, the flow distribution directly coming from the network equations. This model is able to identify and predict the critical paths of the possible cascading failures, given some steady initial condition, with a probabilistic model that allows to explore selectively the future beyond single failures.

The statistical analysis enabled by the proposed model indicates that under normal operation conditions power grid is more robust than one where independent flows occur. This implies that Kirchoff's laws and Ohm's law impose a robustness not present in, say, transportation networks because they force an orderly distribution of flows whereas a transportation network admits a random distribution and the possibility of one that could be disastrous.

The rest of the paper is organized as follows. In Section II we presents the system model and the flow distribution in a power grid network. In Section III we introduce a new stochastic model to determine the statistics of the flows, their changes in case of failures, and the probability they have of overloading lines and therefore propagating more failures,

based on a Markov process model. Note that the branching process introduced by [16], though somewhat similar, is only modeling the number of line that are switched off, without consideration of the location of failures and how the cascading process propagate in the network, which our analysis provides. We introduce metrics that can be monitored to unveil what is the risk of failure and the time margin that is left to perform corrective action in Section III-E. Numerical examples and conclusions (Section IV, V) complete this paper .

II. System Model and Flow Distribution

The *DC power flow* approximation is a standard approach widely used in optimizing flow dispatch and for assessing line overloads (see [18] for more details). Consider a power grid transmission network with n nodes interconnected by m transmission lines. Each network node is associated with an input power P_i which is positive for a generation bus, negative for a load bus, or equal to zero for a transmission substation bus. Each transmission line $l = (i, j)$, between nodes i and j, has line impedance $z_{pr}(l) = r_l + jx_l$, with r_l being the resistance and x_l the reactance. Usually for a high-voltage transmission network, it holds that $x_l \gg r_l$, i.e., the reactance dominates. The *DC power flow* model assumes that $r_l \approx 0$, that the voltage magnitude at all buses approximate their specified base values, i.e., $\|V_i\| \approx 1.0$ (p.u.), and that the angular separation across any transmission line is small enough so that $\sin(\theta_i - \theta_j) \approx \theta_i - \theta_j$. Given a grid containing n_g generation buses and n_l load buses with the injected power vectors as G and $-L$ respectively[1], the network flow equation can be written as follows:

$$P = B'\theta, \tag{1}$$

where $P = [G^T, -L^T]^T$ represents the vector of injected real power and θ the phase angles . B' is defined as

$$B' = A^T diag\,(y_l)\, A, \tag{2}$$

where $y_l = 1/x_l$ is the line admittance; $diag\,(y_l)$ represents a diagonal matrix with entries of $\{y_l, \quad l = 1, 2, \cdots, m\}$. $A := (A_{l,k})_{m\times n}$ is the line-node incidence matrix, arbitrarily oriented, defined as: $A_{l,i} = 1$; $A_{l,j} = -1$, if the l^{th} link is from node i to node j and $A_{l,k} = 0, k \neq i, j$. And the power flow through each transmission line F is:

$$F \quad = diag\,(y_l)\, A\theta. \tag{3}$$

A line is considered as *overloaded* if the power flow through it exceeds the line limit determined by its thermal capacity or static/dynamic stability conditions, i.e., with $|F_l| \geq F_l^{\max}$.

A. Solving the DC Flow Equation

In the DC power flow model (1), the network admittance matrix is approximated as the B' matrix which is a real symmetric matrix by construction. Therefore its eigen-decomposition (EVD) has n linearly independent real eigenvectors:, i.e.

$$B' = \mathbb{V}\mathbf{\Lambda}\mathbb{V}^T, \tag{4}$$

[1]For the sake of brevity, here we take the interconnection buses as load buses with $L = 0$.

where $\mathbb{V}$ is an orthogonal matrix, and Λ is real and diagonal. It is true that usually all the lines are inductive, with $x_l > 0$, in a high-voltage transmission network. Hence all the off-diagonal entries of B' are non-positive and diagonal entries non-negative. Therefore B' can be viewed as a *weighted Laplacian*, which, according to [19], is positive semidefinite and 0 is its smallest eigenvalue. We assume the eigenvalue to be ordered as $\lambda_n \geq \cdots \geq \lambda_2 \geq \lambda_1 = 0$. If the power grid network is connected, 0 is a simple eigenvalue with the corresponding eigenvector $\mathbf{v}_1 = \frac{1}{\sqrt{n}}\mathbf{1}$. The second smallest eigenvalue, $\lambda_2 > 0$, is called the *algebraic connectivity* of the network, which indicates that how closely the nodes in the network are connected together.[2] If the grid network is *disconnected* and divided into $(\hat{k} > 1)$ islands, the B' will have $\hat{k}$ eigenvalues of 0 and $\hat{k} - 1$ is called the *degree of reducibility* of the topology [19]. More details on a disconnected grid can be found in [20].

Applying the pseudo inverse of B' we get the Least Squares (LS) solution to the DC power flow equation:

$$\theta = \mathbb{V}\mathbf{\Lambda}^{\dagger}\mathbb{V}^T P = \sum_{i=\hat{k}+1}^{n} \lambda_i^{-1}\mathbf{v}_i \cdot \xi_i \tag{5}$$

where

$$\xi_i = \mathbf{v}_i^T P, \quad i = 1, 2, \cdots, n$$

are the projection coefficients of P onto the vectors in $\mathbb{V}$ so that P can be written as a linear combination of column vectors in $\mathbb{V}$, i.e.,$P = \sum_{i=1}^{n} \xi_i \mathbf{v}_i$. Here $(\cdot)^{\dagger}$ represents pseudo inverse by taking the reciprocal of each non-zero singular values on the diagonal, leaving the zeros in place, and transposing the resulting matrix. If the power settings is *balanced or feasible*, that is,

$$\xi_i = 0, \qquad \text{for } i = 1, \cdots, \hat{k},$$

(5) gives the exact solution to the DC power flow equation which satisfies $B'\theta = P$, same as that in [17] where the equation is solved by taking inverse of the reduced B' matrix for each isolated subnetwork and setting the angle of the reference node (called *slack bus*) to 0 .

On the other hand, if any ξ_i corresponding to the null space of B' does not equal to zero, it means that the DC power flow equation does not hold, or the power generation and loads are not balanced and the system in fact experiences oscillations in such a situation. And the least square solution by (5) in fact indicates the mean value of the oscillation process.

B. Flow Distribution

Now let us further examine how the coupling structure of a power grid affects the flow distribution on the transmission lines. Define the weighted line-node incidence matrix as

$$\widetilde{A} = \sqrt{y}A \tag{6}$$

[2]In rare cases, some transmission line(s) may carry an capacitive reactance with $x_l < 0$. Hence it is possible that one or more eigenvalues in (4) become negative. So (4) is no longer equivalent to the SVD of the matrix B'. Instead, the latter gives $B' = \mathbb{V}'|\mathbf{\Lambda}|\mathbb{V}^T$, with the pairs of singular vectors from $\mathbb{V}'$ and $\mathbb{V}$ corresponding to a negative eigenvalue differ only by a factor of -1 while the rest pairs of vectors are still identical to each other. We can also generalize the definition of algebraic connectivity to be the second smallest absolute eigenvalues, i.e., $|\lambda_2|$.

where $\sqrt{y} = diag\{\sqrt{y_l}\}$. So that $B' = \widetilde{A}^T \widetilde{A}$. We can therefore derive the following:

Lemma 1: For a given operating condition P and weighted line-node incidence matrix as (6), the vector of flows F in the grid is either equal or it oscillates around the following value:

$$F = \sqrt{y}(\widetilde{A}^T)^\dagger P. \tag{7}$$

Proof: : The proof is omitted in this paper due to the limited space but can be found in the full paper [20]. ■

Lemma 1 shows that the line flows are coupled with the power injections through the matrix $\sqrt{y}(\widetilde{A}^T)^\dagger$: the component vectors in F are in fact the left singular vectors of $\widetilde{A}$ stretched by $\sqrt{y}$ with projection coefficients of $\left(s_i^{-1}\xi_i\right)$.

Note that (7) gives the flow-power sensitivity matrix and can be used to estimate the statistics of line flows given the statistics of injected power(see Section III-B).

III. The Stochastic Model for Cascading Process

A cascade of failures may be triggered when one or more components in the power transmission network are randomly or intentionally brought down. The initial outage results in a re-distribution of line flows in the network, which may in turn cause the flow through some other line(s) to increase and reach the state of overloading. The overloaded lines are prone to fail and be tripped by protective relays after some duration of time, which in turn cause another around of flow re-dispatch. This process continues until no more line outage occurs. The relay settings that require a line in the transmission network to trip are various, e.g., the voltage drops, line overloads, or even some complex stability index. However, here we mainly consider the line tripping events caused by overloading and other random factors like mis-trips of protective relays, human errors, mal-operations or intentional attacks, lightening or unpruned trees, etc, which are among the main reasons that trigger cascading failures.

In this paper a stochastic model based on conditional Markov transition is proposed to study the cascading failures in a power grid, which is able to indicate which part in the network will be under stress and therefore most likely to break down given current network conditions and states. One important purpose of this cascading model is to help discover the most probable and critical evolution path for cascading failures.

A. A Conditional Markov Transition Model for the Cascading Process in Power Grids

First we define the grid state as the vector of line states as $\mathbf{s} = [s_1, s_2, \cdots, s_m]$ and $s_l \in [0,\ 1]$. For each line $s_l = 0$ represents the state that the line is tripped, and $s_l = 1$ that when the line is on, and works normally. So that the admittance of the line at time t can be represented as $y_l(t) = y_l s_l(t)$ and the network admittance matrix is

$$B'(t) = A^T diag\left\{y_l(t)\right\} A. \tag{8}$$

Since $\mathbf{s}(t)$ is an m-dimension binary vector clearly its state space $\mathcal{S}$ contains totally 2^m possible outcomes. Define the stage index h as the total number of tripped lines, with $h = 0, 1, \cdots, m$. The total state space then can be divided into $(m+1)$ subsets, each subset $\mathcal{S}^{(h)}$ with $\binom{m}{h}$ different outcomes respectively. If the system starts from an intact system with normal operating conditions with all 1's in $\mathbf{s}(0)$, we can assume that

$$p\{\mathbf{s}(0)\} = \begin{cases} 1, & \text{if } \mathbf{s}(0) = (1, 1, \cdots, 1) \\ 0, & \text{otherwise.} \end{cases} \tag{9}$$

We then model the random process of the grid state as conditionally Markovian on the evolution process of line flows in the grid network. Given the flow vector evolution over time, the state transition probability is a function of the line transition rates assuming that the relays operate independently.

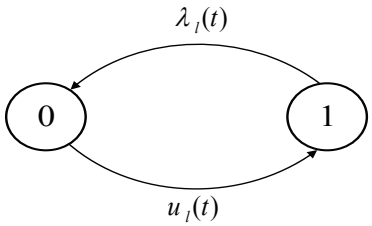

Fig. 1: The line state transition

The line state transition is depicted as in Fig. 1. $\lambda_l(t)$ is the line tripping rate and $\mu_l(t)$ the line restoration rate. $\lambda_l(t)$ is time-varying and depends on the line flow process given current network conditions and states.The line restoration is associated with the reclosing mechanism of the protective relays which are intended to recover from temporary contingencies which exist only for a very short instant. Since the contributive factors to cascading failures are usually persistent, a reclosed line will soon be tripped again and not reclosed. Therefore in the rest of the paper we will ignore the line restoration in our transition model by assuming that $u_l(t) = 0$. That is, $s_l = 0$ can be viewed as an absorbing state. Thus, with $dt = t' - t$ and $0 < dt \ll 1$, we have that

$$\begin{aligned} &p\{s_l(t') = 1 | s_l(t) = 1\} = 1 - \lambda(t)dt \\ &p\{s_l(t') = 0 | s_l(t) = 1\} = \lambda(t)dt \\ &p\{s_l(t') = 1 | s_l(t) = 0\} = 0 \\ &p\{s_l(t') = 0 | s_l(t) = 0\} = 1. \end{aligned} \tag{10}$$

Assuming independent tripping on the lines, the network state $\mathbf{s}(t)$ transition can be obtained by the concatenation of all the line transitions. Define the set of *normally* operating lines in the network as $L_{\mathbf{s}}^n(t) = \{l;\ \ s_l(t) = 1\}$, so the the set of *down* lines is $L_{\mathbf{s}}^d(t) = L^0 \backslash L_{\mathbf{s}}^n(t)$. Let $K(t) = |L_{\mathbf{s}}^n(t)|$ called the network size of the state $\mathbf{s}(t)$. Here $L^0 = \{1, 2, \cdots, m\}$ includes all the transmission lines in an intact system. At the next time instant t' with the state vector as $\mathbf{s}(t')$ with operational lines of $L_{\mathbf{s}}^n(t')$, the set of tripped lines is $T(t, t') = L_{\mathbf{s}}^n(t) \setminus L_{\mathbf{s}}^n(t')$. Hence we have the transition probability as

$$p\{\mathbf{s}(t') | \mathbf{s}(t)\} = \prod_{i \in L_{\mathbf{s}}^n(t')} (1 - \lambda_i(t)dt) \prod_{j \in L_{\mathbf{s}}^n(t) \backslash L_{\mathbf{s}}^n(t,t')} \lambda_j(t)dt \tag{11}$$

Considering dt as infinitesimal, we can omit $o(dt)$ in (11) so

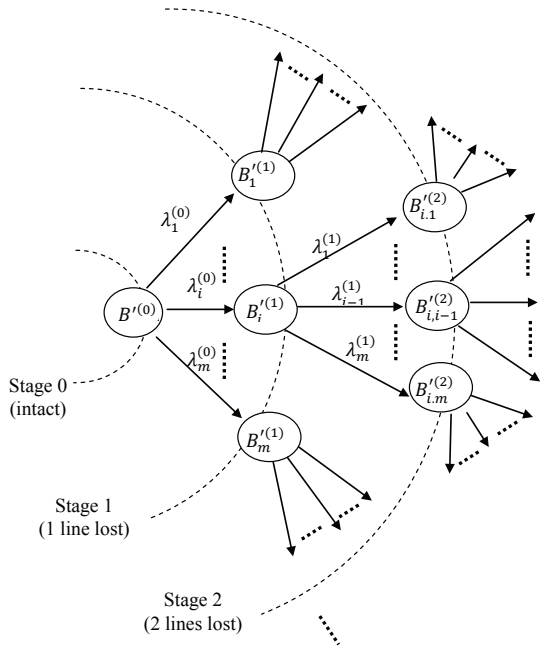

Fig. 2: The Markov transition model for power grid cascading failures.

that,

$$p\{\mathbf{s}(t')|\mathbf{s}(t)\} = \begin{cases} 1 - \sum_{i \in L_{\mathbf{s}}^n(t')} \lambda_i(t)dt, & \text{if } \mathbf{s}(t') = \mathbf{s}(t), \\ \lambda_k(t)dt, & \text{if } T(t,t') = k \in L_{\mathbf{s}}^n(t), \\ 0, & \text{otherwise.} \end{cases} \tag{12}$$

That is, (12) only considers the state transitions with at most one line tripped, i.e., $|T(t,t')| \leq 1$.

The state transition diagram of the cascading failures process in the network is shown in Fig. 2. For the network admittance matrix $B_k'^{(h)}$, h stands for the stage index which is equal to the number of cumulative line trips $h = m - |L_{\mathbf{s}}^n(t)|$ and k indicates the most recently tripped line. For the transition rate $\lambda_l^{(h)}$, h is the stage index of current state while l the possibly tripped line at the next instant. There are two points worth noting here. (1) $\lambda_l(t)$ is time-varying and depends on the line flow process in the grid; in the following subsections we will discuss how λ_l is associated with random contingencies, line overloading, and tripping mechanism. (2) There are overlaps in $B_k'^{(h)}$ in Fig.2, which means that the state transition from some different prior states in fact aim at a same target.

Now we further discuss the overlapping target states in the transition of (12). For the sake of clarity, we will denote a state with its stage index listed explicitly, i.e., as $\mathbf{s}^{(h)}$, for the rest of this subsection. Since we only consider state transitions with at most one line tripped, only $(m-h)+1$ states in $\mathcal{S}$ are *reachable* during the next instant, given the current state. By *reachable* we mean the corresponding transition is associated with a non-zero transition rate in (12). Because $\mathbf{s}^{(h)}(t)$ implies that the grid has $(m-h)$ operating lines, it can arrive at only $(m-h)$ different states in $\mathcal{S}^{(h+1)}$, during the next instant. Given the subset sizes, the overlap ratio of target states for the state transition from $\mathcal{S}^{(h)}$ to $\mathcal{S}^{(h+1)}$:

$$r(h) = \frac{\binom{m}{h}(m-h)}{\binom{m}{h+1}} = h+1. \tag{13}$$

This indicates that given a target state $\mathbf{s}$ from $\mathcal{S}^{(h+1)}$, there are $(h+1)$ different states from $\mathcal{S}^{(h)}$ that can transit to it. Denote this set of *from* states as $\mathcal{F}(\mathbf{s})$ $\left(\subseteq \mathcal{S}^{(h)}\right)$. Therefore the probability of $\mathbf{s}(t') = \mathbf{s}$ can be obtained as

$$\begin{aligned} p\{\mathbf{s}(t') = \mathbf{s}\} = &\sum_{v \in \mathcal{F}(\mathbf{s})} p\{\mathbf{s}(t') = \mathbf{s} |\ \mathbf{s}(t) = \mathbf{v}\}\, p\{\mathbf{s}(t) = \mathbf{v}\} \\ &+ p\{\mathbf{s}(t') = \mathbf{s} |\ \mathbf{s}(t) = \mathbf{s}\}\, p\{\mathbf{s}(t) = \mathbf{s}\}, \end{aligned} \tag{14}$$

with the transition probabilities from (12). For any $\mathbf{v} \in \mathcal{F}(\mathbf{s})$, define the tripped line index as

$$k_{\mathbf{v}}^* = L_{\mathbf{v}}^n \setminus L_{\mathbf{s}}^n, \tag{15}$$

so that the corresponding transition probability will be $p\{\mathbf{s}(t') = \mathbf{s} |\ \mathbf{s}(t) = \mathbf{v}\} = \lambda_{k_{\mathbf{v}}^*} dt$. Therefore (14) becomes

$$\begin{aligned} p\{\mathbf{s}(t') = \mathbf{s}\} = &\sum_{\mathbf{v} \in \mathcal{F}(\mathbf{s})} \lambda_{k_{\mathbf{v}}^*}\ p\{\mathbf{s}(t) = \mathbf{v}\}\ dt \\ &+ \left(1 - \sum_{i \in L_{\mathbf{s}}^n} \lambda_i(t)dt\right) p\{\mathbf{s}(t) = \mathbf{s}\}, \end{aligned} \tag{16}$$

B. Line Overloading Probability

To define the line overloading probability, we need to model the flow as a random process. We use Lemma 1 to express the statistics of the flows as a function of the statistics of the operating conditions next.

Lemma 2: Assume the power injection $P(t) = [G(t)^T \quad -L(t)^T]^T$ has mean and covariance:

$$\mu_P(t) = \begin{bmatrix} \mu_g(t) \\ -\mu_l(t) \end{bmatrix}, \quad C_P(t) = \begin{bmatrix} \Sigma_{gg}(t) & \Sigma_{gl}(t) \\ \Sigma_{lg}(t) & \Sigma_{ll}(t) \end{bmatrix}. \tag{17}$$

Then, the line flows mean and covariances are:

$$\begin{aligned} \mu_F(t) &= \sqrt{y_t}(\widetilde{A}_t^T)^\dagger \mu_P(t) \\ C_F(t) &= \sqrt{y_t}(\widetilde{A}_t^T)^\dagger C_P(t)(\widetilde{A}_t)^\dagger \sqrt{y_t}, \end{aligned} \tag{18}$$

with $\sqrt{y_t} = diag\{\sqrt{y_l(t)}\}$.

Note that usually it is a rational assumption that the injection power at each bus are independent of each other, i.e., the covariance matrix $C_P(t)$ is diagonal. However, the numerical analysis based on (18) indicates that under normal operation conditions the line flows in a power grid are in fact correlated with each other and this correlation makes the grid more robust than one where independent flows occur.

With some necessary direction adjustments in the line-node incidence matrix A, we are able to make sure that $\mu_F(t) \geq 0$. If there exists any $\mu_{F_l}(t) \leq 0$, we only need to reverse the corresponding line direction from $l = (i,j)$ to $l = (j,i)$, which will make the mean value non-negative. Note this line direction adjustment does not cause any change in $B_t'(t)$, as shown in (2). The variance is $\sigma_{F_l} = \sqrt{C_F(l,l)}$.

If $P(t)$ is Gaussian, so is the distribution for $F_l(t)$. In this case, the overloading probability $\rho_l(t) = p\{|F_l(t)| > F_l^{\max}\}$,

for the l^{th} transmission line, as

$$\rho_l(t) = \mathcal{Q}(a_l) + 1 - \mathcal{Q}(b_l) \approx \mathcal{Q}(a_l) \tag{19}$$

in terms of the $\mathcal{Q}$-function $\mathcal{Q}(x) = \int_x^\infty e^{-t^2/2}/(\sqrt{2\pi})dt$ with $a_l = \frac{F_l^{\max} - \mu_{F_l(t)}}{\sigma_{F_l(t)}}$ and $b_l = \frac{-F_l^{\max} - \mu_{F_l(t)}}{\sigma_{F_l(t)}}$. Note that both a_l and b_l, are time-varying. For the sake of brevity, however, we omit the time index in the rest of this paper. The approximation is valid if $\mu_{_F}(t) \gg 0$, since $1 - \mathcal{Q}(b_l) = p\{F_l(t) < -F_l^{\max}\}$ becomes negligible compared to the first term in (19).

Taking a_l as the *normalized distance* of the line flow to its overload threshold, the approximation (19) makes the line overload probability $\rho_l(t)$ fully dependent on a_l.

We can expect that the overload status of line flows in a power grid network might be correlated. Under normal operating conditions, most line flows will stay safely below the line capacities; while during the escalation phase of cascading failures, some of the lines may become overloaded and get tripped within a very short time. We define the *Mahalanobis overload distance* [21] (Mahalanobis 1936) based on the covariance matrix $C_{_F}(t)$ as

$$D_m \;=\; \sqrt{(F^{\max} - \mu_{F(t)})^T C_{_F}^{\dagger}(t)(F^{\max} - \mu_{F(t)})}. \tag{20}$$

which can be viewed as the overload distance of all the lines in the network as a whole. On the other hand, if the line flows are independent of each other, the covariance matrix $C_{_F}(t)$ will become diagonal and the network *Mahalanobis* overload distance be equal to the *Euclidian* overload distance,

$$D_e = \sqrt{\textstyle\sum_l a_l^2}. \tag{21}$$

Obviously we should have $D_m \geq D_e$ under normal operations and we can take the ratio (D_m/D_e) as a correlation indicator for the line overloading.

C. Level Crossing Intervals of the Line Flow Process

Within some time window $[t_0, t_0+T]$, the flow $F_l(t)$ can be considered as a stationary low-pass Gaussian process equal to the sum of its mean, which is deterministic, plus a zero-mean component $v_{_{F_l}}(t)$, that has the same temporal (and spatial) covariance as the flow, $R_{_{F_l}}(\tau)$, i.e., $F_l(t) = \mu_{_{F_l}} + v_{_{F_l}}(t)$. Its power spectrum $\mathbf{S}(\omega)$ is usually bandlimited, that is, $\mathbf{S}(\omega) \approx 0$ for $|\omega| > \widehat{w}$, with $\widehat{w}$ as its largest frequency. Given the flow process on a line $F_l(t)$ with the overloading threshold of $F_l^{\max}$, we can then define the time series of successive up-crossings $t_l^u(i)$ and down-crossing $t_l^d(i)$ instants, i.e. the time instants when the flow $F_l(t)$ crosses the threshold $F_l^{\max}$ from below and those when the flow crosses the threshold from above, respectively, as shown in Fig.3. The corresponding series of crossing intervals, during which $F_l(t) > F_l^{\max}$ and which $F_l(t) \leq F_l^{\max}$, are:

$$\begin{aligned} \tau_l^u(i) &= t_l^d(i) - t_l^u(i) \\ \tau_l^d(i) &= t_l^u(i) - t_l^d(i-1). \end{aligned} \tag{22}$$

$\tau_l^u(i)$ are called *overload* and $\tau_l^d(i)$ the *normal-load intervals*.

Given a_l and ρ_l, the overload and normal-load interval means of the flow process $F_l(t)$ are

$$\bar{\tau}_l^u = \frac{2\pi\rho_l e^{a_l^2/2}}{W}, \quad \bar{\tau}_l^d = \frac{2\pi(1-\rho_l)e^{a_l^2/2}}{W}, \tag{23}$$

where $W = \sqrt{\frac{-R''(0)}{R(0)}}$ is the equivalent bandwidth of the flow process. Hence, from Rice [22], the probability density of an upward level-crossing interval, $\tau > 0$, (i.e., the overload interval in our case) can be approximated as below:

$$f_T(\tau; a_l) \approx \begin{cases} \frac{\pi\tau}{2\bar{\tau}_l^2} \exp\left[-\frac{\pi}{4}\left(\frac{\tau}{\bar{\tau}_l}\right)^2\right], & a_l \gg 1 \\ \frac{1}{\bar{\tau}_l} \exp\left(-\frac{\tau}{\bar{\tau}_l}\right), & a_l \ll -1 \end{cases} \tag{24}$$

where $\bar{\tau}_l$ is the mean sojourn time. Obviously the PDF of a normal-load interval can be approximated as $f_T(\tau; -a_l)$ from (24). Two points are worth noting[22]: a) for a medium-value a_l, say, $a_l \in [-3, 3]$, it is uneasy to obtain an analytical-form $f_T(\tau; a_l)$ which in fact lies between above two limits and is usually estimated by numerical results; b) (24) approximates well only for smaller τ's (compared with its $\bar{\tau}_l$). For larger τ's, the PDF tends to approach $f_T(\tau; a_l) \propto \exp\left(-\frac{\tau}{\bar{\tau}_l}\right)$. Next Section III-D uses $f_T(\tau; a_l)$ to estimate the average line state at the end of each interval, whose accuracy, however, will be shown not dependent on the availability of an analytical-form $f_T(\tau; a_l)$ for a medium-value a_l, or the approximation accuracy for larger τ's. Note that the following analysis within this section are then all based on the assumption of stationarity within some limited time window. In [20], we extend the results to non-stationary conditions.

D. Transition of Line States

Here we derive the line state transition probabilities (see Fig. 1) as a function of the state transition rates $\lambda_l(t)$ (c.f. (10)), and relating these state transition rates to the flow $F_l(t)$ statistics at time t and the overloading threshold $F_l^{\max}$. We further assume that transition rates depend only on the network state but not on the prior history, since the behavior of the relay that trips the line does not have memory in our model. The case of relays with memory, for example, due to repeated attempts of turning the line back on, can be easily handled generalizing the analysis by increasing the number of states, including a certain number of temporary $s_l = 0$ states before the complete shut down. A possible model for the transition rate to state $s_l(t) = 0$ from $s_l(t) = 1$ of the l^{th} line is:

$$\lambda_l(t) = \begin{cases} \lambda_l^*, & t_l^u(i) < t \leq t_l^d(i) \\ \lambda_l^0, & t_l^d(i-1) < t \leq t_l^u(i), \end{cases} \tag{25}$$

where λ_l^* is related with the relay settings specified to trip off an overloaded line within some time threshold which can be different for each line; and λ_l^0 represent the line tripping rate caused by random contingencies which is usually trivial compared with λ_l^*, i.e., $\lambda_l^0 \ll \lambda_l^*$. Fig. 3 shows how the overload/normal load intervals determine the transition rate $\lambda(t)$. From this model and the statistics derived in the previous section for the sojourn time we have:

Lemma 3: The probability $p\{s_l(t) = 1\}$ of the l^{th} line state

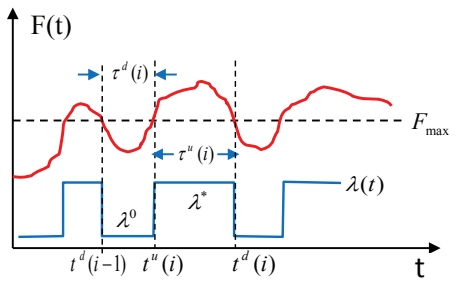

Fig. 3: The overload intervals of $F(t)$ and the transition rate of $\lambda(t)$

at the end of an overload and a normal-load interval are:

$$\begin{aligned} p\left\{s_l\left(t_l^d(i)\right)=1\right\} &= e^{-\lambda_l^*\tau_l^u(i)} \\ p\left\{s_l\left(t_l^u(i)\right)=1\right\} &= e^{-\lambda_l^0\tau_l^d(i)}. \end{aligned} \tag{26}$$

Proof: The proof is omitted in this paper due to the limited space but can be found in the full paper [20]. ■

E. Time Measure of Safety

Utilizing the probability density of level-crossing intervals and the statistics of line state transitions, we recognize the expectation of line state probability at the end of each overload interval:

Lemma 4:

$$\begin{aligned} \alpha_l = & \quad E\left\{p\left\{s_l\left(t_l^d(i)\right)=1\right\}\right\} \\ = & \begin{cases} 1-\lambda_l^*\bar{\tau}_l^u \exp\left(\frac{(\lambda_l^*\bar{\tau}_l^u)^2}{\pi}\right) erfc(\frac{\lambda_l^*\bar{\tau}_l^u}{\sqrt{\pi}}), & a_l \gg 1 \\ 1/\left(\lambda_l^*\bar{\tau}_l^u+1\right), & a_l \ll -1 \\ c_1\left[1-\lambda_l^*\bar{\tau}_l^u \exp\left(\frac{(\lambda_l^*\bar{\tau}_l^u)^2}{\pi}\right) erfc(\frac{\lambda_l^*\bar{\tau}_l^u}{\sqrt{\pi}})\right]+ \\ \quad + c_2\left[1/\left(\lambda_l^*\bar{\tau}_l^u+1\right)\right], & a_l \text{ medium-value} \end{cases} \end{aligned} \tag{27}$$

$$\begin{aligned} \beta_l = & \quad E\left\{p\left\{s_l\left(t_l^u(i)\right)=1\right\}\right\} \\ = & \begin{cases} 1-\lambda_l^0\bar{\tau}_l^d \exp\left(\frac{(\lambda_l^0\bar{\tau}_l^d)^2}{\pi}\right) erfc(\frac{\lambda_l^0\bar{\tau}_l^d}{\sqrt{\pi}}), & a_l \ll -1 \\ 1/\left(\lambda_l^0\bar{\tau}_l^d+1\right), & a_l \gg 1 \\ 1-\lambda_l^0\bar{\tau}_l^d, & a_l \text{ medium-value} \end{cases} \end{aligned} \tag{28}$$

where $c_1,\ c_2 > 0$ are interpolation coefficients with $c_1 + c_2 = 1.0$; $c_1 \to 1$ as $a_l \gg 1$; satisfying $c_2 \to 1$ as $a_l \ll -1$.

Proof: The proof is omitted in this paper due to the limited space but can be found in the full paper [20]. ■

Hence we can have the expected time for the line to stay connected as follows:

Lemma 5: Given the overload probability ρ_l of the l-th line, the level crossing density γ_l at $F_l^{\max}$, and the line tripping rates λ_l^* for an overload line and λ_l^0 caused by random contingencies, the expected time for the line to stay safe is:

$$\mathcal{T}_l = (\bar{\kappa}_l - 1)/\gamma_l + E\{\Delta t_l\}, \tag{29}$$

where

$$\bar{\kappa}_l \ = \ \left[(1+\beta_l)-(\beta_l-\alpha_l)\rho_l\right]/(1-\alpha_l\beta_l) \tag{30}$$

is the expected number of crossings after which the l^{th} line finally gets tripped; and

$$E\{\Delta t_l\} = \left[\Delta T_l^* + \Delta T_l^0\right]/(1-\alpha_l\beta_l) \tag{31}$$

is the mean duration of the last *interval, with* $\Delta T_l^* = (1-\alpha_l)\left[\beta_l + (1-\beta_l)\rho_l\right]/\lambda_l^*$ *and* $\Delta T_l^0 = (1-\beta_l)\left[1-(1-\alpha_l)\rho_l\right]/\lambda_l^0$.

Proof: The proof is omitted in this paper due to the limited space but can be found in the full paper [20]. ■

$\mathcal{T}_l$ can be viewed as a measure for the line to stay "safe" and $\min_l \mathcal{T}_l(t_0)$ is a global metric for the safety of the grid under current network condition and

$$l^* = \arg\ \min_l \mathcal{T}_l \tag{32}$$

indicates the line under the most distress. If the network transfers from one state to another, however, the $\mathcal{T}_l$'s all change, because the flows will be redistributed, and most likely this minimum will shrink further and happen at a different line.

F. Normalized Overload Distance and Minimum Safety Time

Using the approximation of (19), we can see that the overloading probability ρ_l, the expected line non-trip probabilities α_l and β_l at the end of each overload or normal-load intervals, the average crossing rate γ_l, the average crossing intervals $\bar{\tau}_l^u$ and $\bar{\tau}_l^d$, the expected number of crossings before line trips $\bar{\kappa}_l$ as well as the expected safety time $\mathcal{T}_l$, can all be defined as functions of one variable a_l, the normalized distance of the line flow $F_l(t)$ to it overload threshold. If a_l is positive and large, the line flow stays safely away from its overload threshold, i.e, lightly-loaded. However, if a_l gets smaller and closer to zero or even becomes negative, it implies that its mean approaches or exceeds beyond the overloading threshold $F_l^{\max}$.

Now we further illustrate how these quantities relate with the normalized overload distance a (the line index is omitted here). Fig. 4 shows a sample set of the curves evaluated with $w = 10^{-3}$ Hz, $\lambda^* = .0017$ Hz, and $\lambda^* = 7.7 \cdot 10^{-11}$ Hz. Fig. 4(a) depicts the overload probability curve and the probabilities of $\alpha(a)$ and $\beta(a)$; as a decreases, i.e., the line flow turns more and more overloaded, $\alpha(a)$ will gradually decrease to zero; on the other hand, $\beta(a) = 1.0$ most of the cases except the extremely lightly-loaded condition. This is interesting because when $a \gg 1$, the normal-load interval grows to be very lengthy (longer than years), which consequently drives the line state at the end of the interval $\beta(a) \to 0$. Fig. 4(b) shows that the crossing rate $\gamma(a)$ achieves its maximum $\gamma^{\max} = w/\pi$ at $a = 0$; and when $|a| \gg 1$, the crossing rate becomes extremely small. Fig. 4(c) indicates that $\bar{\tau}^u(a)$ grows as a decreases while $\bar{\tau}^d(a)$ grows as a increases; if $a \gg 1$, both ρ_l and γ approach zero while $\bar{\tau}^u(a)$ approaches the limit of $\sqrt{2\pi}/|aw|$; on the other had, if $a \ll -1$, both $(1-\rho_l)$ and γ approach zero while $\bar{\tau}^d(a)$ approaches the same limit $\sqrt{2\pi}/|aw|$. Fig. 4(d) shows that $\bar{\kappa}(a)$ is monotonic-increasing with a except that an abrupt drop to 1.0, beyond $a \approx \sqrt{\ln\left[(w/\lambda^0)^2/(40\pi)\right]}$ exactly the same location where $\beta(a)$ goes down to 0 very sharply. This tells us that when neglecting the extremely lightly-loaded conditions the line flows always tend to have less crossings before the trip happens. This is very important for analyzing non-stationary flow process in the next section. Fig.4(e)(f) present the curves of $E\{\Delta t(a)\}$ and $\mathcal{T}(a)$: both grow monotonically with a. And

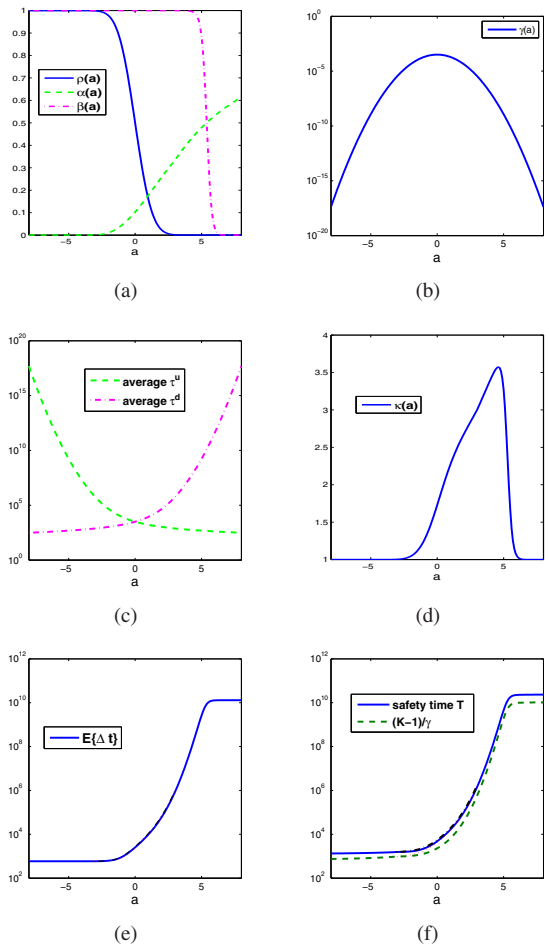

(a) (b) (c) (d) (e) (f)

Fig. 4: The quantities versus the normalized distance to the overload threshold a: (a) the overloading probability $\rho(a)$, the line non-trip probabilities $\alpha(a)$ and $\beta(a)$; (b) the average crossing rate $\gamma(a)$; (c) the average interval length $\bar{\tau}^u(a)$ and $\bar{\tau}^d(a)$; (d) the expected number of crossing before tripping $\bar{\kappa}(a)$; (e) the average time before tripping in the last interval $E\{\Delta t\}$; (f) the safety time $\mathcal{T}(a)$.

it is very clear that as $a \gg 1$, $\mathcal{T}(a)$ approaches $1/\lambda^0$, while as $a \ll -1$, $\mathcal{T}(a)$ approaches $1/\lambda^*$.

Based on the above analysis one can clearly see that the most critical lines in a network in the sense of a shortest safety time can also be identified as the line with the smallest overload distance a_l given current operating condition, That is

$$l^* = \arg \min_l \mathcal{T}_l = \arg \min_l a_l. \tag{33}$$

The definition of $a_l = \frac{F_l^{\max} - \mu_{F_l}}{\sigma_{F_l}}$ tells that the value of a_l depends on three factors, i.e., the line capacity $F_l^{\max}$, the mean of the line flow μ_{F_l}, and the corresponding variance σ_{F_l}.

IV. Simulation and Experiment Results

We experiment with the proposed stochastic model on the IEEE 300 bus system. The IEEE-300 system is a synthesized network from the New England power system and has a topology with 300 nodes and 411 links. The initial operating equilibrium and conditions, $(G(0), L(0), \theta(0), F(0))$ are taken or derived from the power flow solution of the system data from [23]. Taking the mean of $P(0)$ as $\mu_P(0) = [G(0)^T, -L(0)^T]^T$, We set the standard deviation of the loads as $\sigma_L = \delta|L(0)|$, but ignore the variance in G. For simplicity, we assume that the loads and generation are statistically independent of one other. The line capacities are set as $F^{\max} = \max\{\eta|F(0)|,\ 2.0(p.u.)\}$ with $\eta = 1.20$. Here we take $F(0)$ as the rational flow distribution under normal operating conditions and assume that the line capacity allows a 20% load increase [24]. The minimum of line capacity is set to be 2.0 p.u. so that the vibration in the lines which usually carry small flows will not cause frequent line trips. Analysis on the load record from realistic power grids [25] has shown that the load process can be approximated as a low-pass Gaussian process with an equivalent bandwidth of $W \approx 10^{-5}$Hz and the load data assumes an extremely strong correlation within a time window about $T = 30$ mins. Since the flow process in a grid can be seen as a linear projection from the load process, we can apply the equivalent bandwidth W and the corresponding stationary time window length T to the flow processes in the grid. Table I below summarizes all the simulation parameters in our experiments. The random contingency probability of an electric power grid is usually by design extremely small, except under some very special conditions such as when a thunderstorm occurs in the area, $\lambda^0(t)$ may become non-trivial during a very short temporary interval. Here we set $\lambda^0 = 7.7 \cdot 10^{-11}$ for all the lines which accounts for a contingency rate of about 1-in-a-year. For simplicity of simulation, the line tripping rate is assumed to be constant for all the lines as $\lambda^* = 1.92 \cdot 10^{-2}$.

TABLE I: Simulation Parameters for the Cascading Process in the IEEE 300 Bus System

T	30 mins	λ^*	$1.92 \cdot 10^{-2}$
W	10^{-5} Hz	λ^0	$7.70 \cdot 10^{-11}$
δ	0.07	η	1.20

Under the given operating conditions as described above and with parameters in Table I, the IEEE-300 system has a minimum safety time of $\min_l \mathcal{T}_l \approx 105$ hours. In order to trigger and observe a cascading process, we have to manually introduce some random contingencies within a short instant at the beginning of the simulation (i.e., tripping the line 115-131 at $t = 10$ min). Fig. 5 shows the evolution process of cascading failures under some stress conditions. The increasing curve of cumulative line trips is comparable to those recorded in [16]. During the fast escalation phase, the cumulative line trips grows exponentially with an exponent of 0.3178 $\min^{-1}$. And this corresponds to multiplication of the cumulative line trips by a factor of 1.37 every minute. Please note that here we display a most severe case of cascading evolution during which no actions have been taken to stop the propagation of flow overloads. In realistic operation, some protective actions such as intentional load shedding or islanding may be executed, in the middle of this process, to slow and finally calm down the process.

Fig. 6 displays the normalized overload distance a_l, the minimum safety time T_l, the overload margin $(F_l^{\max} - \mu_{F_l})$ and the flow variance σ_{F_l} of all the lines in the network after

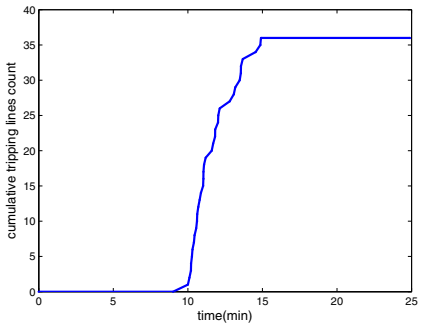

Fig. 5: The cumulative line trips in a cascading process: the IEEE-300 system

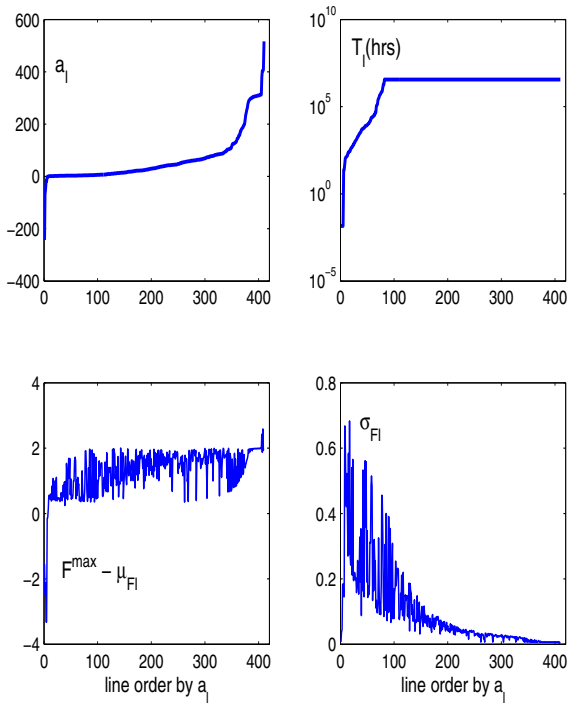

Fig. 6: The a_l, T_l, $(F_l^{\max} - \mu_{F_l})$ and σ_{F_l} after line 109-130 tripped: the IEEE-300 system

line 115-131 tripped and all the data points have been sorted according to a_l in the ascending order. The line 115-131 is an important backbone link which initially carries a 3.78 (p.u) load flow and is among the most heavily loaded lines in the network. It can be seen from Fig. 6 that tripping the line 115-131 cause the mean flow on some lines to go beyond their line capacities and result in some negative overload distances and very small T_l. Therefore additional line trips can be expected to happen very quickly. Fig. 6 verifies that the minimum safety time of each line T_l grows monotonically as a_l increases and it also indicates that the variance in a line flows seems to be a more dominant factor than the overload margin $(F_l^{\max} - \mu_{F_l})$ to determine the corresponding normalized overload distance since the former has a clear descending trend when ordered by a_l.

Fig.7 shows the Mahalanobis overload distance $D_m(t)$ and the Euclidean overload distance $D_e(t)$ of the whole network and their ratios $D_m(t)/D_e(t)$ during the above cascading process. From the definition of $D_m(t)$ and $D_e(t)$ in Section III-B, we know that $D_m(t)$ represents the overall distance of the whole network from its overload boundary, while $D_e(t)$ is a network overload distance evaluated based on the assumption that all the flows in the network are independent random variables. It can be seen that during this cascading process $D_m(t)$ has a clear trend of dropping as more and more lines get tripped in the system (except some irregular bumps), which means the remaining network tends to get closer to its overload boundary. On the other hand, the Euclidean overload distance $D_e(t)$ manifests a very different trend: it tends to grow higher instead of lower. From the flow redistribution analysis we already know that line trips in a power grid do not always cause line flow increases; it can cause some line flows to decrease as well. Since $D_e(t)$ is evaluated by assuming that all the flows in the network are independent of each other, the lightly-loaded lines with large overload distance, resulted from previous line trips, in the remaining network are in fact given more weights in the evaluation of $D_e(t)$. Therefore D_e can get larger during a cascading process. However, this may not truly reflect the overload status of the whole network. On other hand, it is interesting to notice that the ratio $D_m(t)/D_e(t) > 1.0$ during the process, i.e., the the Mahalanobis overload distance is always larger than the Euclidean overload distance. This means that the line flows in a power grid correlate together therefore act much more safely than a network whose line flows are independent of each other. In fact the latter is the worst case in terms of flow-overload vulnerability. Another worth-noting discovery is that the ratio of $D_m(t)/D_e(t)$ gets smaller during the cascading process, which implies that the correlation of the line flows becomes weaker as more lines have been removed from the network. And it can be expected that in case a large portion of lines have been tripped and the whole network divided into islands, this ratio may approach 1.0, that is, the line flows become independent random variables.

V. Conclusions

In this paper we first examine the flow distribution in a power grid network which follows a set of significantly different rules from those of information or traffic networks, and explain why graphic analysis cannot apply directly on a power grid network. Then we propose a stochastic cascading model based on conditional Markov transition. Some of its advantages include: (1) it takes into account the uncertainty in the load settings and thus the uncertainties in the generation and line flows; (2) it correctly captures the stochastic process of the evolution of cascading failures in a power grid with regard to real time signal (i.e., instead of stage numbers); (3) it is able to indicate which parts of the system are under most stresses therefore most likely to break down in the next time interval. This is useful to identify and predict the critical paths of the possible cascading failures, given some steady initial condition, with a probabilistic model that allows to explore selectively the future beyond single failures. We introduce metrics that can be monitored to unveil what is the risk of

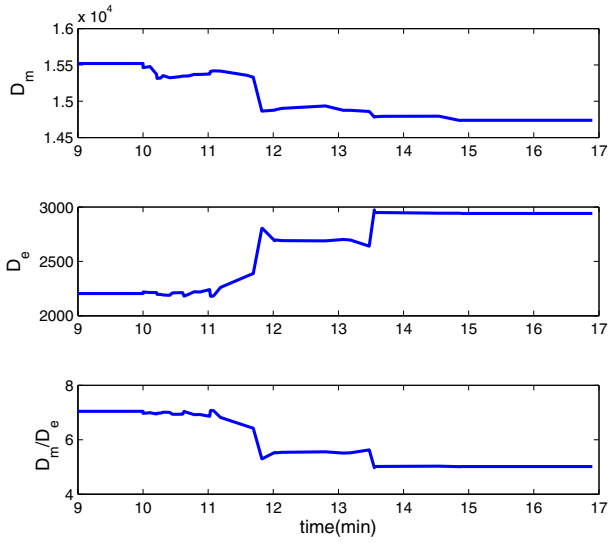

Fig. 7: The Mahalanobis and Euclidean overload distance during the cascading process: the IEEE-300 system

failure and the time margin that is left to perform corrective action.

The experiments on the proposed model with the IEEE 300-bus system have shown the evolution process of cascading failures with the cumulative line trips increasing exponentially with regard to time, with a comparable pattern as those of the historical records from some realistic power grids.

The experimental analysis also indicates that the line flows in a power grid are correlated therefore act much more safely than a network comprised of independent line flows. During the cascading process, the correlation of the line flows becomes weaker as more lines are removed from the network. As a result the overall distance from the overload boundary, defined by the Mahalabonis overload distance, may be decreased.

VI. ACKNOWLEDGMENTS

This work was funded by the UIUC TCIPG Project sponsored by DOE under the Award DE-OE0000097. The authors thank Mahnoosh Alizadeh and Saeed Bagheri for the suggestion to apply the Line Outage Distribution Factor to flow distribution computation.

REFERENCES

[1] M. Rosas-Casals, S. Valverde, and R. Solé, "Topological vulnerability of the european power grid under erros and attacks," *International Journal of Bifurcations and Chaos*, vol. 17, no. 7, pp. 2465–2475, 2007.

[2] R. Solé, M. Rosas-Casals, B. Corominas-Murtra, and S. Valverde, "Robustness of the european power grids under intentional attack," *Physics and Society (physics.soc-ph), (on line): http://arxiv.org/abs/0711.3710*, 2007.

[3] Z. Wang, A. Scaglione, and R. J. Thomas, "The node degree distribution in power grid and its topology robustness under random and selective node removals," in *1st IEEE International Workshop on Smart Grid Communications (ICC'10SGComm)*, Cape Town, South Africa, May 23 2010.

[4] H. Xiao and E. M. Yeh, "Cascading link failure in the power grid: A percolation-based analysis," *CoRR*, 2010.

[5] P. Hines, E. Cotilla-Sanchez, and S. Blumsack, "Topological models and critical slowing down: Two approaches to power system blackout risk analysis," in *the 44th Hawaii International Conference on System Sciences (HICSS-44)*, Hauai, Hawaii, USA, Jan. 4 – 7 2011.

[6] A. Motter and Y. Lai, "Cascade-based attacks on complex networks," *Phys. Rev. E*, vol. 66, p. 065102(R), 2002.

[7] P. Holme and B. J. Kim, "Vertex overload breakdown in evolving networks," *Phys. Rev. E*, vol. 65, no. 6, p. 066109, Jun. 2002.

[8] P. Crucitti, V. Latora, and M. Marchiori, "Model for cascading failures in complex networks," *Phys. Rev. E*, vol. 69, p. 045104(R), 2004.

[9] R. Kinney, P. Crucitti, R. Albert, and V. Latora, "Modeling cascading failures in the north american power grid," *The European Physical Journal B*, vol. 46, no. 1, pp. 101–107, 2009.

[10] Y. Xia, J. Fan, and D. Hill, "Cascading failure in wattsstrogatz small-world networks," *Physica A: Statistical Mechanics and its Applications*, vol. 389, no. 6, pp. 1281–1285, Mar. 2010.

[11] J. Wang and L. Rong, "Cascade-based attack vulnerability on the us power grid," *Safety Science*, vol. 47, pp. 1332–1336, 2009.

[12] I. Dobson, B. A. Carreras, V. E. Lynch, and D. E. Newman, "An initial model for complex dynamics in electric power system blackouts," in *34th Hawaii International Conference on System Sciences*, Maui, Hawaii, Jan. 2002.

[13] B. A. Carreras, V. E. Lynch, I. Dobson, and D. E. Newman, "Critical points and transitions in an electric power transmission model for cascading failure blackouts," *Chaos*, vol. 12, no. 4, pp. 985–994, 2002.

[14] I. Karamitsos and K. Orfanidis, "An analysis of blackouts for electric power transmission systems," *Proceedings of World Academy of Science, Engineering and Technology*, vol. 12, pp. 290–293, Mar. 2006.

[15] Z. Bao, Y. Cao, G. Wang, and L. Ding, "Analysis of cascading failure in electric grid based on power flow entropy," *Physics Letters A*, vol. 373, no. 34, pp. 3032–3040, Aug. 2009.

[16] I. Dobson, B. A. Carreras, and D. E. Newman, "Branching process models for the exponentially increasing portions of cascading failure blackouts," in *38th Hawaii International Conference on System Sciences*, Big Island, Hawaii, Jan. 2005.

[17] J. D. Glover and M. S. Sarma, *Power System Analysis and Design*. Brooks/Cole, 2001.

[18] A. Wood and B. Wollenberg, *Power System Generation, Operation and Control*. New York: Wiley, 1984.

[19] M. Fiedler, "A property of eigenvectors of nonnegative symmetric matrices and its application to graph theory," *Czechoslovak Mathematical Journal*, vol. 25, no. 4, pp. 619–633, 1975.

[20] Z. Wang, A. Scaglione, and R. J. Thomas, "A stochastic approach to studying cascading failures in electric power grids," *(available on line) http://arxiv.org/submit/265679*, 2011.

[21] P. C. Mahalanobis, "On the generalised distance in statistics," *Proceedings of the National Institute of Sciences of India*, vol. 2, no. 1, p. 4955, 1936.

[22] S. O. Rice, "Distribution of the duration of fades in radio transmission:gaussian noise model," *Bell Syst. Tech. J.*, vol. 37, p. 581635, May 1958.

[23] Power systems test case archive [Online],Available: http://www.ee.washington.edu/research/pstca/.

[24] R. D. Dunlop, R. Gutman, and P. P. Marchenko, "Analytical development of loadability characteristics for ehv and uhv transmission lines," *IEEE trans on Power Apparatus and Systems*, vol. 98, no. 2, p. 606617, March 1979.

[25] National Grid, http://www.nationalgrid.com/uk/Electricity/Data/Demand+Data/.